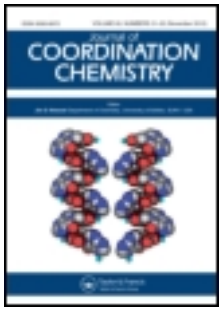

Journal of Coordination Chemistry
Publication details, including instructions for authors and subscription information:
http://www.tandfonline.com/loi/gcoo20

Syntheses, characterizations, and antimicrobial activities of binuclear ruthenium(III) complexes containing 2-substituted benzimidazole derivatives

B. Roopashree [a] , V. Gayathri [a] , A. Gopi [b] & K.S. Devaraju [b]
[a] Department of Chemistry , Central College Campus, Bangalore University , Bangalore 560 001 , India
[b] Department of Biotechnology , Jnanabharathi Campus, Bangalore University , Bangalore 560 056 , India
Accepted author version posted online: 18 Sep 2012.Published online: 01 Oct 2012.

To cite this article: B. Roopashree , V. Gayathri , A. Gopi & K.S. Devaraju (2012) Syntheses, characterizations, and antimicrobial activities of binuclear ruthenium(III) complexes containing 2-substituted benzimidazole derivatives, Journal of Coordination Chemistry, 65:22, 4023-4040, DOI: 10.1080/00958972.2012.731050

To link to this article: http://dx.doi.org/10.1080/00958972.2012.731050

Journal of Coordination Chemistry
Vol. 65, No. 22, 20 November 2012, 4023–4040

Syntheses, characterizations, and antimicrobial activities of binuclear ruthenium(III) complexes containing 2-substituted benzimidazole derivatives

B. ROOPASHREE†, V. GAYATHRI*†, A. GOPI‡ and K.S. DEVARAJU‡

†Department of Chemistry, Central College Campus, Bangalore University, Bangalore 560 001, India
‡Department of Biotechnology, Jnanabharathi Campus, Bangalore University, Bangalore 560 056, India

(*Received 11 June 2012; in final form 27 August 2012*)

Binuclear ruthenium(III) complexes $[RuX_3L]_2 \cdot nH_2O$ (X = Cl, L = L^1, L^2, L^3; $n = 1$, L^4 and L^5, X = Br; L = L^3), $[RuX_3L_{1.5}]_2 \cdot nH_2O$ (X = Br, L = L^1; $n = 0$, L^4; $n = 6$ and L^5; $n = 10$), and $[RuX_3L_2]_2$ (X = Br, L = L^2) have been isolated by treatment of hydrated RuX_3 (X = Cl/Br) in acetone with 2-(2′-aminophenylbenzimidazole) (L^1), 2-(3′-aminophenylbenzimidazole) (L^2), 2-[(3′-N-salicylidinephenyl)benzimidazole] (L^3), 2-(3′-pyridylbenzimidazole) (L^4), and 2-(4′-pyridylbenzimidazole) (L^5) in acetone. The complexes were characterized by elemental analysis, conductivity and magnetic susceptibility measurements, IR, electronic, EPR, and mass spectral studies. The complexes were dimeric; based on analytical and spectral studies, an octahedral geometry was proposed for the complexes. The synthesized complexes were screened against Gram-positive and Gram-negative bacteria and fungi.

Keywords: Ruthenium(III) complexes; 2-Substituted benzimidazoles; Spectral studies; Antimicrobial activity

1. Introduction

The benzimidazole ring is an important pharmacophore. A variety of benzimidazoles such as thiabendazole and flubendazole (anthelmintic), omeprazole and lansoprazole (antiulcerative) and astemizole (antihistaminic) are in use. The chemistry and pharmacology of benzimidazoles are of interest to medicinal chemistry [1, 2] because of their ability to interact with a range of different enzymes and receptors. Substituted benzimidazoles exhibit pharmacological activities, such as anti-inflammatory, antioxidant, gastroprotective, and antiparasitic activities [3]. Transition metal complexes of biologically important ligands are more effective than uncoordinated heterocycles. Ruthenium(III) complexes represent a new family of promising metal-based anticancer drugs that offer the potential of reduced toxicity compared to antitumor platinum(II) complexes used currently. Ruthenium compounds offer medicinal applications as an

*Corresponding author. Email: gayathritvr@yahoo.co.in

ISSN 0095-8972 print/ISSN 1029-0389 online
http://dx.doi.org/10.1080/00958972.2012.731050

alternative to platinum-based antitumor drugs for treatment of cancer cells that are resistant to cisplatin and its analogs since ruthenium has the ability to mimic iron in binding to certain biological molecules, rate of ligand exchange, and the range of accessible oxidation states [4]. Ruthenium complexes with bisbenzimidazole derivatives display potent cytotoxicity against ovarian carcinoma cells [5, 6]. Ruthenium(III) complexes of Schiff-base ligands are useful catalysts in reactions such as hydrogenation, oxidation, carbonylation and hydroformylation [7–12]. Transition metal systems in which metal ions are linked by a bridging ligand can differ significantly with regard to the nature and/or extent of metal–metal electronic interactions [13]. Here, we report the syntheses, spectroscopic characterizations, and antimicrobial activities of dimeric ruthenium(III) complexes of biologically important 2-substituted benzimidazoles (figure 1).

2. Experimental

2.1. *Materials, methods, and equipment*

All reagents used were of analytical grade. N-heterocycles, 2-(2′-aminophenyl benzimidazole), 2-(3′-aminophenyl benzimidazole), 2-(3′-pyridyl benzimidazole), and 2-(4′-pyridyl benzimidazole) (L^1, L^2, L^4, and L^5) were prepared as per literature methods [14]. Hydrated $RuCl_3$ and $RuBr_3$ were procured from Johnson Matthey Chemicals limited. The solvents used were purified according to standard procedure [15]. *Ampicillin* and *fluconazole* were procured from Ranbaxy, India.

Microanalyses were carried out on a Finnegan Eager 300 elemental analyzer. IR (nujol mull) spectra were recorded on a Shimadzu FTIR 8400s and far-IR spectra were recorded on a Thermo Nicolet 6700 model. Electronic spectra were recorded on a Shimadzu UV 3101PC spectrophotometer. FAB mass spectra were recorded on a JEOL SX102 Mass Spectrometer using argon/xenon as the FAB gas and *m*-nitrobenzyl alcohol as the matrix and ESI-MS on a Thermo LCQ Deca XP MAX. Molar conductivity measurements were made on a Systronic conductivity meter 304-cell type CD-10. Determination of magnetic susceptibilities were carried out by Faraday's method and variable temperature magnetic susceptibility measurements were carried out on a vibrating sample magnetometer, Lakeshore VSM 7410. Biological activities of the N-heterocycles and complexes were carried out by the agar diffusion method.

2.2. *Syntheses of ligands*

2.2.1. L^1, L^2, L^4, and L^5. L^1, L^2, L^4, and L^5 were prepared by condensation of orthophenylene diamine with corresponding organic acid using polyphosphoric acid as a condensing agent at 240°C for 6 h. The resulting mixture was poured into ice cold water and neutralized with 15% $NaOH/Na_2CO_3$ solution. The solids obtained were filtered and recrystallized in alcohol.

2.2.2. L^3, 2-[(3′-N-salicylidinephenyl)benzimidazole]. A new Schiff base, 2-[(3′-N-salicylidinephenyl)benzimidazole] was prepared by condensation of methanolic solution of L^2 with salicylaldehyde at refluxing temperature for 6 h. The reaction mixture was

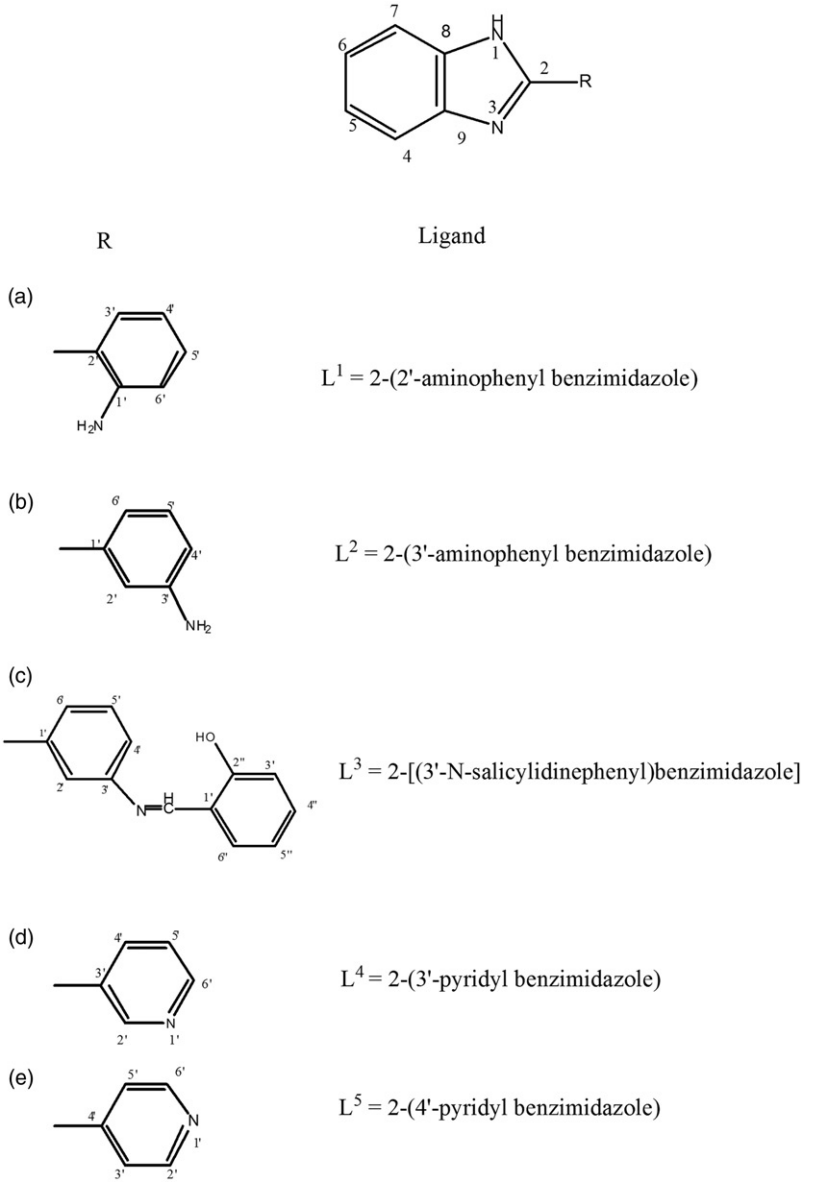

Figure 1. Structures of ligands.

concentrated to get a yellow compound. The solid was filtered, dried, and recrystallized in methanol. Yield: 76%; m.p. 235°C.

2.3. *Syntheses of the complexes*

$[RuX_3L]_2 \cdot nH_2O$ (X = Cl, L = L^1, L^2, L^4,or L^5, $n = 0$; L = L^3, X = Cl or Br, $n = 2$), $[RuBr_3L_{1.5}]_2 \cdot nH_2O$ (L = L^1, $n = 0$; L = L^4, $n = 6$; L = L^5, $n = 10$), and $[RuBr_3L_2^2]_2$.

About 1 mmol of RuX_3 (X = Cl/Br) in acetone (10 mL) was refluxed with 2 mmol of ligand (L = L^1, L^2, L^3, L^4 and L^5) in 10 mL acetone for 6 h. Green/brown/reddish brown compounds were formed. The solids were filtered, washed with methanol/ether, and dried *in vacuo*. Yield: 50–70%.

3. Results and discussion

RuX_3 (X = Cl/Br) reacts with L^1, L^2, L^3, L^4, and L^5 in 1 : 2 mole ratio in acetone to yield green/brown/reddish brown complexes, $[RuX_3L]_2 \cdot nH_2O$ (X = Cl, L = L^1, L^2, L^4, or L^5, $n = 0$; X = Cl or Br, L = L^3, $n = 2$), $[RuBr_3L_{1.5}]_2 \cdot nH_2O$ (L = L^1; $n = 0$, L = L^4; $n = 6$ and L^5; $n = 10$), and $[RuX_3L_2]_2$ (X = Br, L = L^2). $[RuBr_3L^4_{1.5}]_2$ and $[RuBr_3L^5_{1.5}]_2$ were soluble in common organic solvents such as acetone and alcohol whereas other complexes were sparingly soluble in common organic solvents but soluble in DMF and DMSO. The conductivity measurements were carried out in 10^{-3} mol L^{-1} solution in DMF/DMSO. The molar conductance values were 24–49 Ω^{-1} cm^2 mol^{-1}. The observed values were not high enough to be characterized as 1:1 electrolytes, but these values fall within the acceptable range for non-electrolytes [16]. The higher conductivity values may be due to partial replacement of Cl^-/Br^- in the complex by strong donor solvents. Thermogravimetric analyses for $[RuX_3L^3]_2 \cdot 2H_2O$ (X = Cl/Br), $[RuBr_3L^4_{1.5}]_2 \cdot 6H_2O$, and $[RuBr_3L^5_{1.5}] \cdot 10H_2O$ were carried out to 300°C in nitrogen at a heating rate of 15°C per minute to analyze the nature of water associated with these complexes. All four complexes lost water within 100°C, indicating the presence of lattice water. Thermogravimetric analysis was repeated after drying the complexes in vacuum by heating for 48 h. The results are in accord with the composition of the complexes as determined by elemental analyses. The physical properties and analytical data of the compounds are listed in table 1.

Table 1. Physical properties and analytical data of the complexes.

Complex	Color	m.p./d.p. (°C)	Λ (Ω^{-1}cm^2 mol^{-1})	μ (B.M.)	Found (Calcd) (%)		
					C	H	N
$[RuCl_3L^1]$	Green	235	34	0.8	37.45 (37.38)	2.66 (3.07)	9.09 (8.80)
$[RuBr_3L^1_{1.5}]$	Green	>280	23	1.9	36.61 (35.70)	2.76 (2.52)	9.94 (9.63)
$[RuCl_3L^2]$	Green	>280	49	0.9	37.05 (37.50)	2.45 (3.07)	9.05 (8.80)
$[RuBr_3L^2_2]$	Green	>280	24	1.4	41.82 (41.29)	3.44 (2.92)	11.63 (11.11)
$[RuCl_3L^3] \cdot H_2O$	Brown	>280	38	1.6	44.70 (44.58)	3.60 (3.80)	8.40 (7.78)
$[RuBr_3L^3] \cdot H_2O$	Brown	240	49	1.8	35.20 (35.74)	2.40 (2.55)	6.10 (6.25)
$[RuCl_3L^4]$	Green	>280	27	1.6	35.70 (35.79)	2.89 (2.25)	10.80 (10.44)
$[RuBr_3L^4_{1.5}] \cdot 3H_2O$	Reddish brown	235	39	1.7	31.32 (31.45)	3.63 (2.86)	8.78 (9.17)
$[RuCl_3L^5]$	Green	>280	29	1.2	35.70 (35.79)	2.62 (2.25)	10.25 (10.44)
$[RuBr_3L^5_{1.5}] \cdot 5H_2O$	Reddish brown	220	43	1.9	29.75 (29.88)	3.15 (3.27)	8.03 (8.71)

3.1. *IR spectral studies*

The IR spectral data of the ligands and the complexes were recorded as nujol mulls (table 2). The spectra of the complexes are similar to that of uncoordinated N-heterocycles except for minor shifts in the position of the peaks. Free L^1, L^2, L^3, L^4, and L^5 display υ_{N-H} of benzimidazole at 3379, 3174, 3157, 3165, and 3169 cm^{-1}, respectively; υ_{N-H} of NH_2 in L^1 were twin peaks at 3170 and 3143 and L^2 at 3350 cm^{-1} [17]. In complexes of L^1, υ_{N-H} of benzimidazole and NH_2 merged and appeared as a broad peak at 3177–3188 cm^{-1}. Complexes of L^2 display a broad peak at 3109–3166 and 3170 cm^{-1} assigned to υ_{N-H} of benzimidazole and υ_{N-H} of NH_2. The ruthenium complexes of L^4 and L^5 display υ_{N-H} of benzimidazole at 3103–3188 cm^{-1} and $\upsilon_{C=N}$ of benzimidazole and pyridine at 1609–1630 cm^{-1}. The shift in $\upsilon_{C=N}$ in spectra of the

Table 2. Electronic, ESR, and far-IR spectral data of the complexes.

Compound	Electronic spectral data λ_{nm}[a]	d→d Transitions		ESR g[b] $g_\parallel$	ESR g[b] $g_\perp$	Far-IR (cm^{-1}) $\nu_{Ru-X(b)}$ X = Cl/Br	Far-IR (cm^{-1}) $\nu_{Ru-X(t)}$ X = Cl/Br
L^1	316(3407), 354(25,575)	–	–	–	–	–	–
$[RuCl_3L^1]$	301(43,243), 336(22,244)	537(5257)	675(1804)	–	1.89	275	312
$[RuBr_3L^1_{1.5}]$	302(54,414), 310(46,983)	512(1938), 589(1729)	712(3108)	2.08	1.99	–	245
L^2	300(11,760), 309(10,942), 332(3808)	–	–	–	–	–	–
$[RuCl_3L^2]$	300(52,253), 322(36,813), 345(16,171)	537(4952)	664(1859)	$g_{av} = 2.4$			249
$[RuBr_3L^2_2]$	307(41,255), 325(28,065)	555(3016)	675(1879)	2.14	1.99	–	241
L^3	309(31,747), 325(22,499), 353(11,092)	–	–	–	–	–	–
$[RuCl_3L^3]\cdot H_2O$	308(71,632), 321(54,731), 365(18,516)	560(1609)	670(4953)	2.04	–	258	288, 294
$[RuBr_3L^3]\cdot H_2O$	309(77,704), 323(51,267), 347(21,003)	547(4355)	688(1697)	2.25	2.02	211	253
L^4	308(19,299), 320(14,508)	–	–	–	–	–	–
$[RuCl_3L^4]$	312(53,321), 329(38,511)	461(7842)	671(3105)	2.14, 2.05	–	257	309
$[RuBr_3L^4_{1.5}]\cdot 3H_2O$	313(76,897), 332(53,471)	471(6981)	680(468)	$g_{av} = 2.02$			210
L^5	311(18,085), 325(13,390)	–	–	–	–	–	–
$[RuCl_3L^5]$	312(44,576), 329(32,379)	460(8157)	680(1471)	2.05	–	250	303
$[RuBr_3L^5_{1.5}]\cdot 5H_2O$	325(76,152), 358(46,439)	435(11,129)	700(1226)	2.05, 1.80	–	214	238

[a]ε values in parentheses ($dm^3\,mol^{-1}$), [b]at 77 K.

complexes containing pyridine-based ligands, L^4 and L^5, suggests coordination of Ru(III) through tertiary nitrogen of benzimidazole and pyridine. L^3 exhibited υ_{N-H} of benzimidazole and υ_{O-H} of salicylidine moiety at 3157 cm^{-1}. Ruthenium(III) complexes of L^3 display υ_{N-H} of benzimidazole at 3170 and υ_{O-H} of salicylidine moiety and lattice water together as a broad peak at 3400 cm^{-1} [18]. υ_{C-N} and δ_{N-H} in all the complexes were at 3110 cm^{-1}. The IR spectral data of the complexes suggest that the ligands bind to ruthenium(III) *via* tertiary nitrogen of benzimidazole. In complexes of L^1 and L^2, shift in the position of υ_{N-H} of NH_2 and in complexes of L^3, shift in azomethine peak suggest coordination of these groups to ruthenium(III).

The far-IR spectra of the chloro complexes display peaks due to bridging υ_{Ru-Cl} at 250–280 cm^{-1} and terminal υ_{Ru-Cl} at 230–290 cm^{-1}, indicating the presence of both bridging and terminal chlorides. Bromo complexes of L^3, L^4, and L^5 exhibited $\upsilon_{Ru-Br(t)}$ around 250 and $\upsilon_{Ru-Cl(b)}$ around 210 cm^{-1} [19] whereas bromo complexes of L^1 and L^2 displayed peaks corresponding only to $\upsilon_{Ru-Br(t)}$, indicating the absence of bridging bromides.

3.2. *Electronic spectral studies*

Electronic spectra of the ligands and their ruthenium(III) complexes were recorded in DMF (table 2). Low-spin ruthenium(III) is a d^5 system with a ground state $^2T_{2g}$ and the first excited doublet levels in order of increasing energy are $^2A_{2g}$ and $^2A_{1g}$ arising from a $t_{2g}^4\ e_g^1$ configuration. The spectra of free ligands displayed intense bands around 300 and 400 nm which were assigned to $\pi \rightarrow \pi^*$ and $n \rightarrow \pi^*$ transitions, respectively. Spectra of the ruthenium(III) halo complexes containing L^1, L^2 and L^3 also exhibited moderately intense bands at 660–715 nm and around 512–560 nm which were assigned to $^2T_{2g} \rightarrow {}^4T_{1g}$ and $^2T_{2g} \rightarrow {}^4T_{2g}$, respectively.

Spectra of the ruthenium complexes containing L^4 and L^5 in addition to ligand bands showed another prominent band at 460–560 nm due to ligand-to-metal charge transfer and a weaker d–d band appeared as a shoulder at 530 nm characteristic of low-spin Ru(III) with octahedral geometry [20–25].

3.3. *Magnetic moment and EPR spectral studies*

The room temperature magnetic moment values of the ruthenium(III) complexes containing L^3, L^4, and L^5 were 1.4–1.9 B.M., consistent with low-spin d^5 octahedral ruthenium(III) with one unpaired electron. The magnetic moment values of chloro complexes of ruthenium(III) containing L^1 and L^2 at room temperature were less than 1 B.M. Hence variable temperature magnetic susceptibility measurements have been carried out for these two chloro complexes from 0 to 300 K (figures 2 and 3). The effective magnetic moment values for these complexes were low at 50 K and increased with rise in temperature, revealing quenching of the unpaired spins. The lowering of magnetic moment with temperature may be attributed to antiferromagnetic coupling between two Ru(III) centers through bridging chloride or due to lower symmetry ligand fields [26]. Similar values were observed for binuclear ruthenium(III) complexes reported by others [27–29]. Variable temperature magnetic moment measurements of binuclear copper(II) complexes of m-aminophenyl benzimidazole (L^2) reported

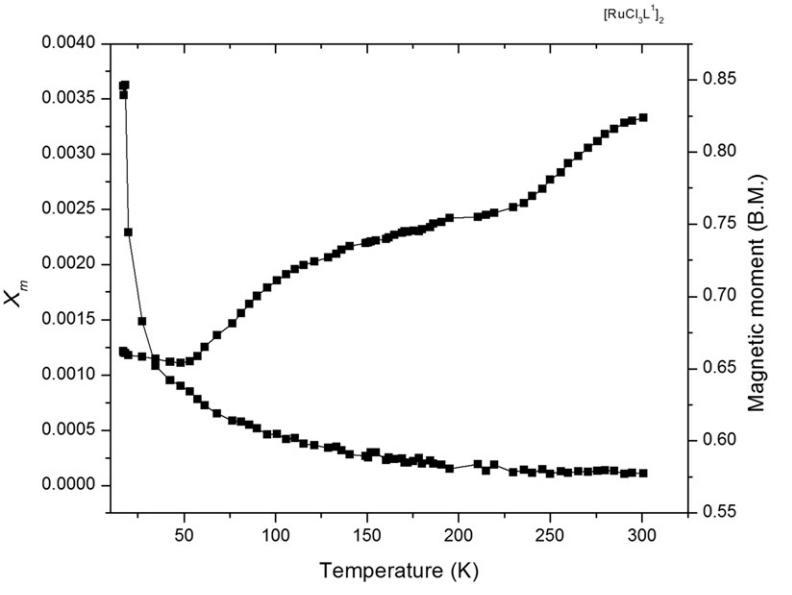

Figure 2. Variation in magnetic susceptibility with temperature (K) for $[RuCl_3L^1]_2$.

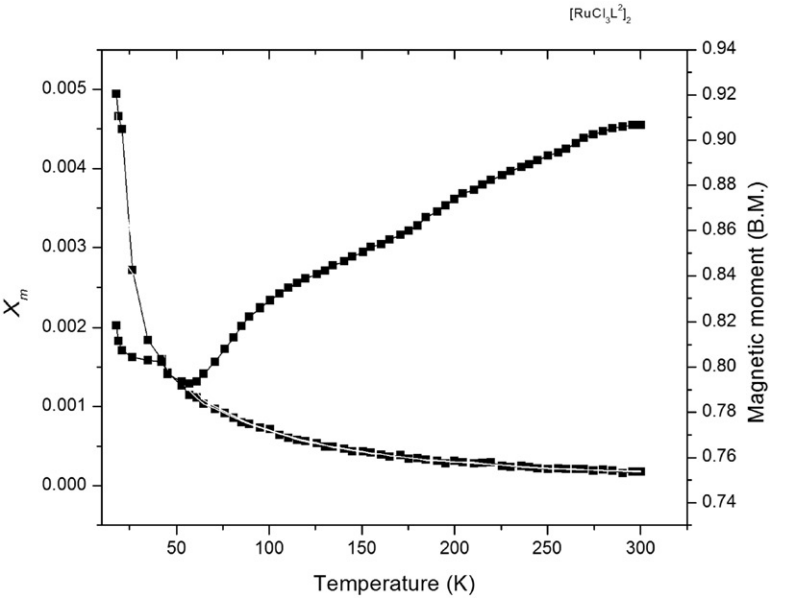

Figure 3. Variation in magnetic susceptibility with temperature (K) for $[RuCl_3L^2]_2$.

earlier [30] revealed the presence of antiferromagnetic coupling between two Cu(II) ions through bridged halides.

X-band ESR spectra of powdered samples of ruthenium(III) complexes have been recorded at ambient temperature and 77 K (table 2). The spectral profiles were typical

of axial type ($g_{\parallel} > g_{\perp}$) implying a $d_{x^2-y^2}$ ground state. The spectral features resemble those of six-coordinate octahedral ruthenium(III) complexes [31]. ESR spectra of Ru(III) chloro complexes of L^1 and L^3 exhibited only one peak with $g_{\parallel}$ of 1.89 and 2.04, respectively. Ruthenium bromo complexes of L^1, L^2, and L^3 exhibited two peaks with g-values of 2.08–2.25 ($g_{\parallel}$) and $g_{\perp}$ (1.99–2.02). Ruthenium complexes of L^5 and chloro complex of L^4 exhibited $g_{\parallel}$-values of 1.80–2.05. ESR signals corresponding to $g_{\perp}$ were centered around 1.95. The $g_{\parallel}$-values less than 2.3 (table 2) for the complexes indicated that the complexes possessed considerable covalent character in the metal–ligand bond.

The ESR spectra of $[RuCl_3L^2]_2$ and $[RuBr_3L^4_{1.5}]_2$ showed a $g_{\perp}$ hyperfine structure with six-line splitting arising due to the nuclear spin of ruthenium ($I = 5/2$), the hyperfine splitting constant (A) being 88 G. The splitting of signal has been attributed to interaction of the unpaired electron with the metal nuclei.

3.4. *Mass spectral studies*

Mass spectra of the ruthenium(III) complexes support the binuclear nature of the complexes [32]. The ESI mass spectra of the ruthenium(III) complexes exhibited peaks corresponding to $Ru_2Cl_6L^1_2$ ($m/z = 834$), $Ru_2Br_6L^1_3$ ($m/z = 1309$), $Ru_2Cl_6L^2_2$ ($m/z = 834$), $Ru_2Br_6L^2_4$ ($m/z = 1518$), $Ru_2Cl_6L^3_2$ ($m/z = 1042$), $Ru_2Br_6L^3_2$ ($m/z = 1308$), $Ru_2Cl_6L^4_2$ ($m/z = 805$), $Ru_2Br_6L^4_3$ ($m/z = 1267$), $Ru_2Cl_6L^5_2$ ($m/z = 805$), and $Ru_2Br_6L^5_3$ ($m/z = 1266$) which supported the binuclear nature of all the complexes. Isotope pattern (figure 4) for representative complexes such as $Ru_2Cl_6L^1_2$, $Ru_2Br_6L^2_4$, $Ru_2Cl_6L^3_2$, and $Ru_2Br_6L^3_2$ had been carried out and they displayed intensity ratios consistent with the calculated isotopic distributions for such binuclear complexes (isopro 3.0), supporting formation of binuclear complexes [33, 34]. The fragmentation patterns of $Ru_2Br_6L^1_3$, $Ru_2Cl_6L^4_2$, and $Ru_2Br_6L^4_{1.5}$ are depicted in "Supplementary material" section, which showed that the decomposition of these complexes finally led to ligand peak $m/z = 210$ and $m/z = 195$ corresponding to 2-aminophenyl benzimidazole and 3-pyridyl benzimidazole, respectively.

4. Stereochemistry

The elemental analyses and IR spectral studies indicate that ligand is coordinated to ruthenium(III). TGA data indicate the presence of lattice water in some complexes. Mass spectral studies support binuclear ruthenium complexes. Electronic spectra of the complexes were similar to those of six-coordinate octahedral ruthenium(III) complexes. Magnetic susceptibility measurements indicate that the complexes are low-spin d^5 with one unpaired electron. Based on these studies, distorted octahedral geometry is proposed for the complexes (figure 5).

L^1 is chelating bidentate in chloro complex and both bridging and chelating in bromo complex. The far-IR spectrum of the chloro complex indicates the presence of both bridging and terminal chloride whereas bromo complex exhibited peaks due to terminal bromides. Hence for these complexes, binuclear structure with chloro bridges for $[RuCl_3L^1]_2$ and bridging L^1 for bromo complex are suggested (figure 5a and b).

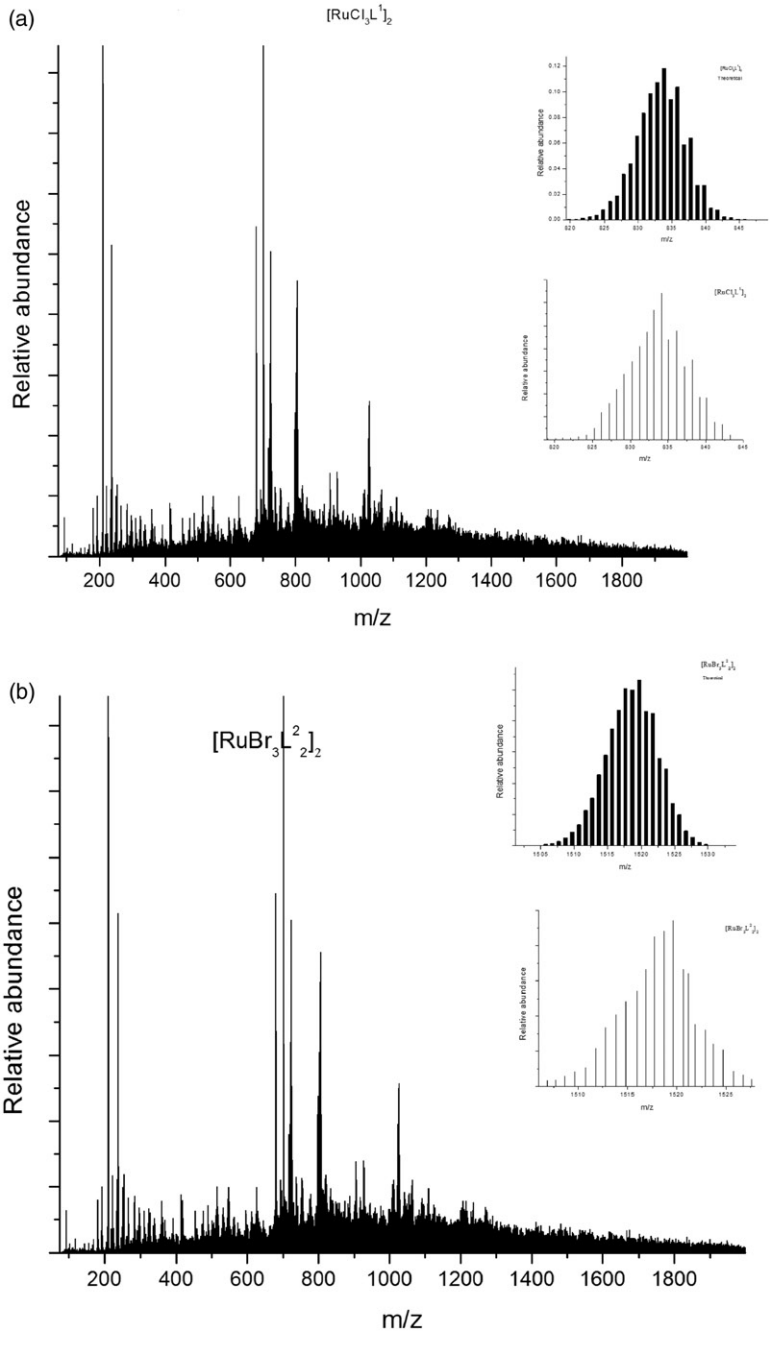

Figure 4. Isotope patterns for (a) $[RuCl_3L^1]_2$, (b) $[RuBr_3L_2^2]_2$, (c) $[RuCl_3L^3]_2$, and (d) $[RuBr_3L^3]_2$.

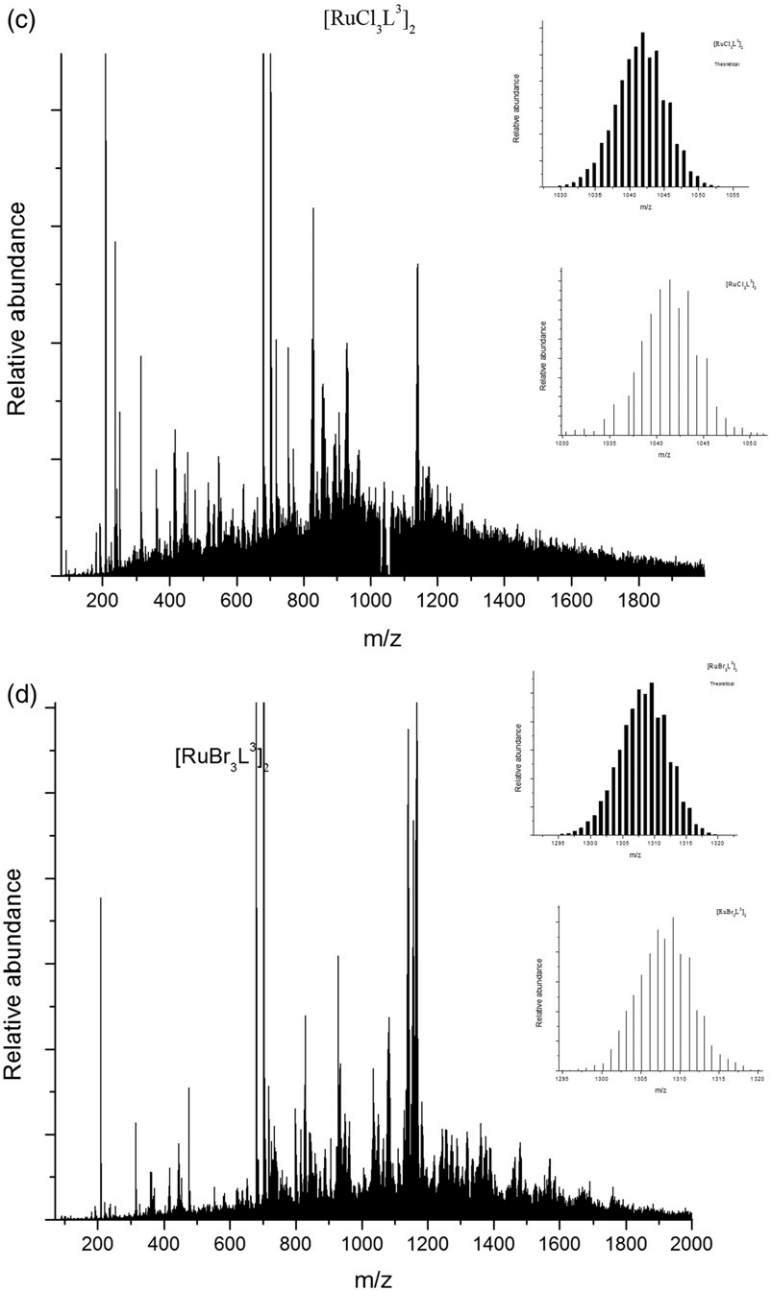

Figure 4. Continued.

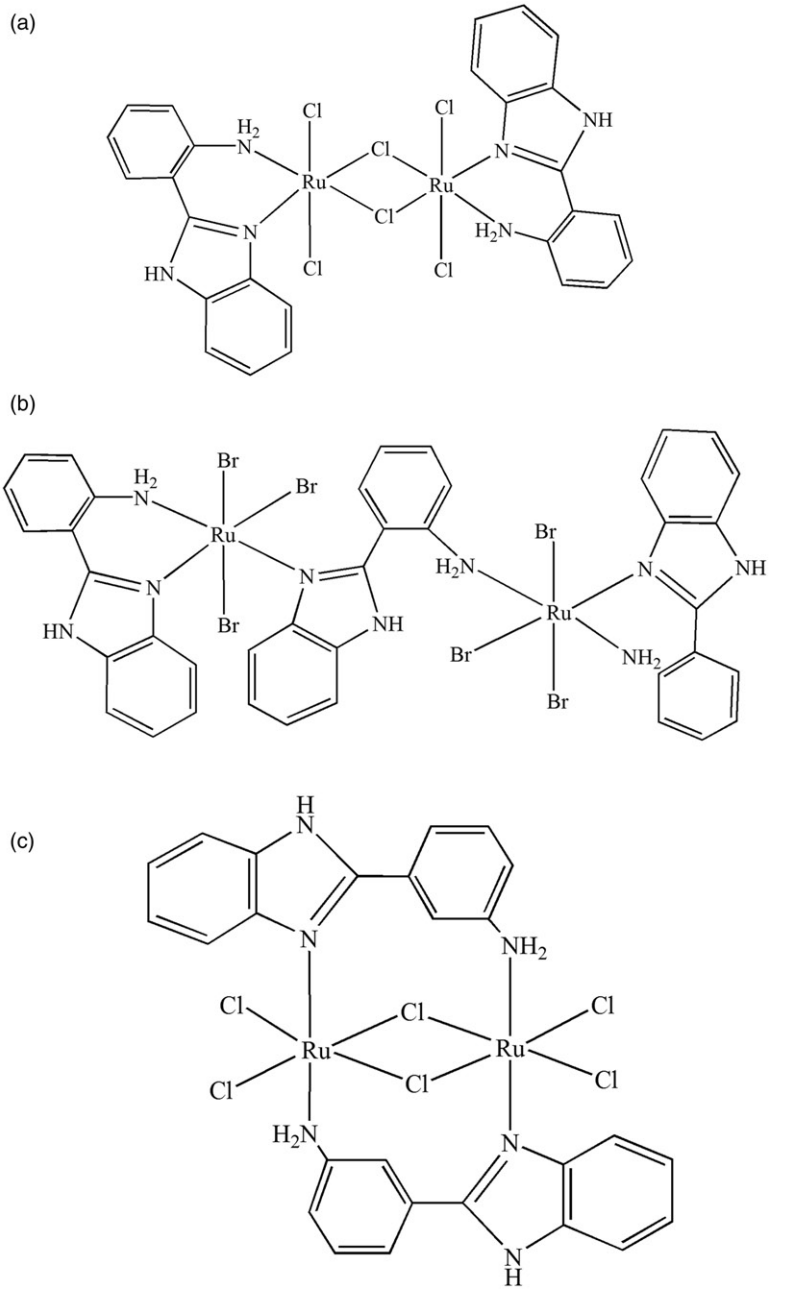

Figure 5. Proposed structures for (a) $[RuCl_3L^1]_2$, (b) $[RuBr_3L^1_{1.5}]_2$, (c) $[RuCl_3L^2]_2$, (d) $[RuBr_3L^2_2]_2$, (e) $[RuX_3L^3]_2$; X = Cl/Br, (f) $[RuCl_3L^4]_2$, (g) $[RuBr_3L^4_{1.5}]_2$, (h) $[RuCl_3L^5]_2$, and (i) $[RuBr_3L_{1.5}]_2$.

(d)

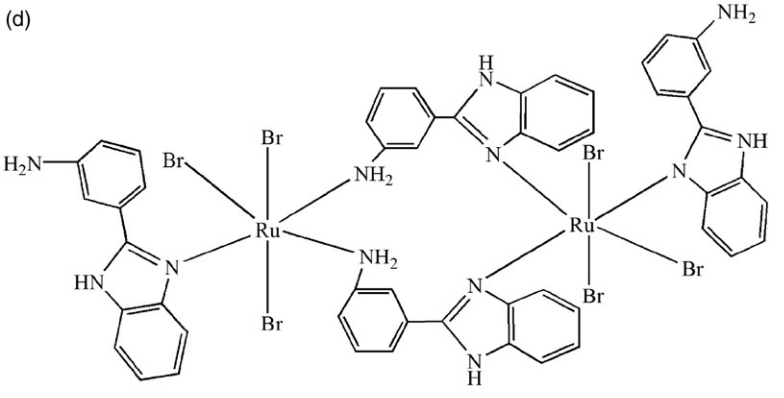

(e)

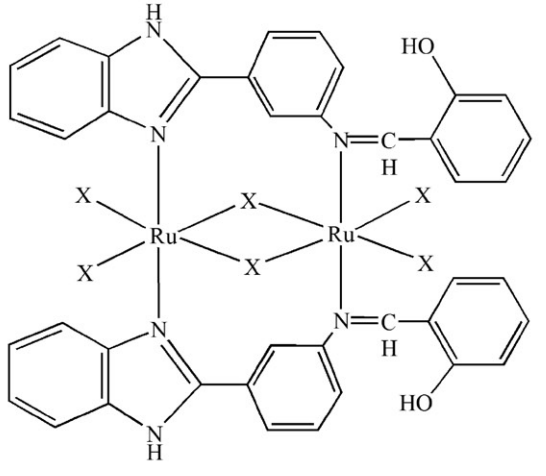

X = Cl/Br

(f)

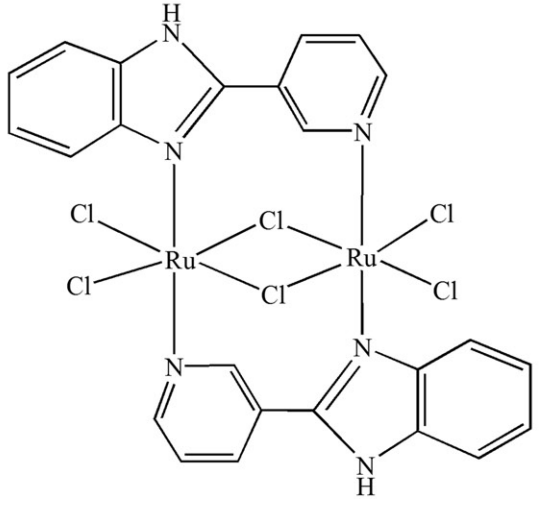

Figure 5. Continued.

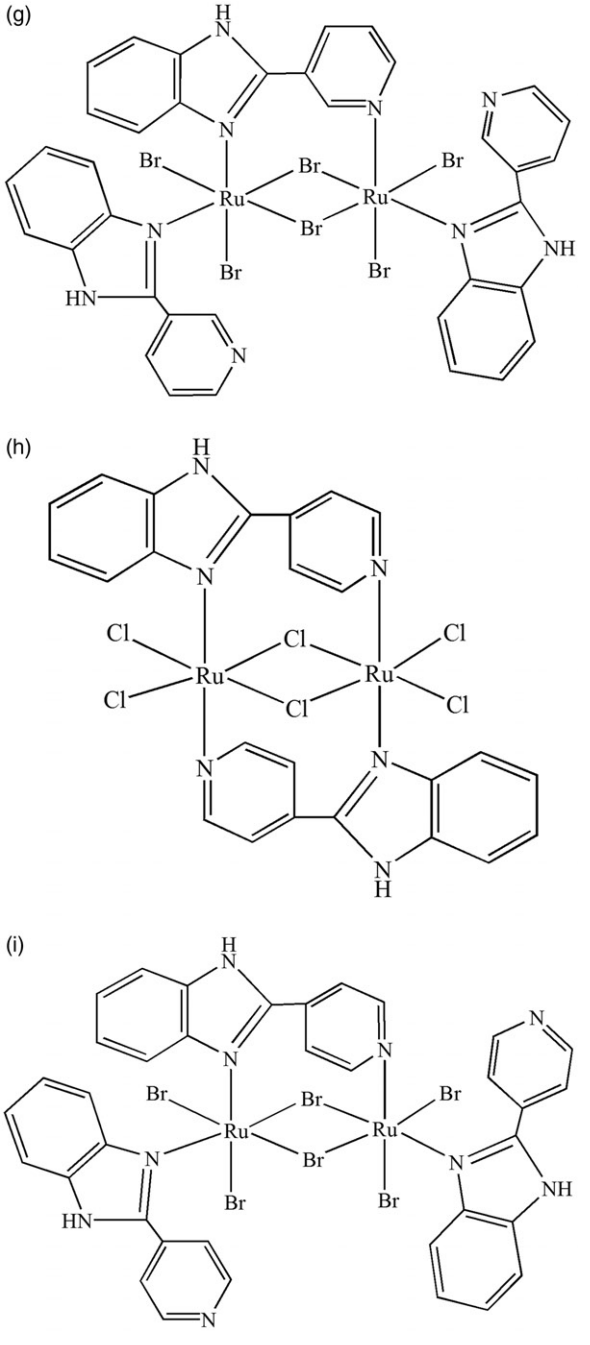

Figure 5. Continued.

Far-IR spectrum of ruthenium(III) chloro complex of L^2 exhibited the presence of both bridging and terminal chlorides. Hence, a binuclear structure with two chloro bridges and L^2 as bridging bidentate are suggested for $[RuCl_3L^2]_2$ (figure 5c). The far-IR spectrum of the bromo complex of L^2 exhibited peaks only due to terminal bromides analyzing as $[RuBr_3L^2_2]_2$. Hence a binuclear structure with two L^2 as bridging bidentate ligands and the other two as monodentate are suggested (figure 5d).

Far-IR spectra of ruthenium complexes with L^3 exhibited peaks due to bridging and terminal halides. Hence a binuclear structure with bridging bidentate ligand coordinating through tertiary nitrogen of benzimidazole and azomethine nitrogen with halogen bridges were assigned (figure 5e).

The far-IR spectra of chloro complexes of L^4 and L^5 exhibited peaks due to bridging and terminal chlorides. Hence, a binuclear structure with bridging bidentate ligands coordinating through pyridine nitrogen and tertiary nitrogen of benzimidazole with two chloro bridges were assigned (figure 5f and h).

Far-IR spectra of bromo complexes of L^4 and L^5 exhibited peaks due to bridging and terminal bromides, analyzing as $[RuBr_3L_{1.5}]_2$ ($L = L^4$ or L^5). Hence a binuclear structure with two ligands monodentate and one bridging bidentate with two bromo bridges were suggested (figure 5g and i).

5. Biological activity

Free ligands, their metal complexes, metal salts, control (DMSO), and the standard drugs ampicillin and fluconazole were screened against bacteria *Staphylococcus aureus*, *Bacillus aureus*, *Escherichia coli,* and *Salmonella typhi* and fungi, *Candida albicans* and *Aspergillus niger* by the agar diffusion method (table 3). The stock solution was prepared by dissolving 10 mg mL^{-1} of the compounds in DMSO. Stock solution was diluted to get 50, 150, 200, and 250 ppm concentrations. The nutrient agar was prepared by dissolving peptone, beef extract, sodium chloride, dextrose, and agar in 1000 mL of distilled water. The mixture was autoclaved at 121°C for 15 min at pH 7.4 and 15 lb pressure per in^2. The mixture was cooled to 45°C and then dispended into sterilized petri dishes, allowed to solidify and then used for inoculation. Fresh cultures of microorganisms were prepared separately by adding 6 g of peptone, 1.5 g of beef extract, 1 g of dextrose, 15 g of agar, and 5 g of sodium chloride in 1000 mL of distilled water and allowed to solidify. 50, 150, 200, and 250 ppm of sterilized solutions were used for the application in the well. Standard drug solution and DMSO control were also poured into separate wells in each plate. The petri dishes were covered and incubated at 37°C for 24 h for antibacterial activity and 28°C for 48 h for antifungal activity. Zone inhibitions were observed and average three readings were recorded. The percentage activity index data for the ligand and metal complexes were calculated as follows:

$$\%\text{Activity index} = \frac{\text{Zone of inhibition by test compound (diameter)}}{\text{Zone of inhibition by standard (diameter)}} \times 100.$$

Table 3. Antibacterial and antifungal activities of the ligands, complexes, and standard drug.

	Antibacterial activity zone of inhibition (mm)										Antifungal activity									
	E. coli					*S. typhi*					*C. albicans*					*A. niger*				
Compound	50 ppm	150 ppm	200 ppm	250 ppm	% Activity index	50 ppm	150 ppm	200 ppm	250 ppm	% Activity index	50 ppm	150 ppm	200 ppm	250 ppm	% Activity index	50 ppm	150 ppm	200 ppm	250 ppm	% Activity index
L^1	2	2	3	4	21	2	2	4	5	26	3	4	7	8	38	na	na	na	na	–
$[RuCl_3L^1]$	7	9	9	11	58	3	4	7	8	42	3	5	8	10	48	2	5	8	10	48
$[RuBr_3L^1_{1.5}]$	6	6	7	11	58	2	3	4	5	26	2	4	7	12	57	0	4	6	8	38
L^2	3	3	4	4	21	2	3	3	4	21	3	5	8	9	43	4	7	11	15	71
$[RuCl_3L^2]$	6	6	8	16	84	5	5	6	7	37	6	9	12	14	67	na	na	na	na	–
$[RuBr_3L^2_2]$	0	0	0	1	–	5	6	9	9	47	7	12	14	16	76	3	9	15	16	76
L^3	1	1	2	3	16	na	na	na	na	–	4	5	6	8	38	na	na	na	na	–
$[RuCl_3L^3]\cdot H_2O$	na	na	na	na	–	4	5	6	7	37	3	4	7	10	48	0	1	2	3	14
$[RuBr_3L^3]\cdot H_2O$	3	6	7	8	42	2	3	4	5	26	4	6	9	13	62	2	3	4	5	24
L^4	1	2	4	5	26	2	3	4	5	26	2	4	5	7	33	na	na	na	na	–
$[RuCl_3L^4]$	5	6	7	9	47	na	na	na	na	–	2	6	9	12	57	2	3	5	5	24
$[RuBr_3L^4_{1.5}]\cdot 3H_2O$	2	3	5	6	32	na	na	na	na	–	2	8	10	14	67	0	1	1	2	09
L^5	2	4	4	5	26	2	3	5	6	32	3	4	5	6	29	na	na	na	na	–
$[RuCl_3L^5]$	9	10	11	12	63	na	na	na	na	–	5	8	12	15	71	1	1	2	3	14
$[RuBr_3L^5_{1.5}]\cdot 5H_2O$	5	5	6	8	42	4	5	6	6	32	6	9	13	15	71	1	2	3	4	19
$RuCl_3$	1	4	5	6	32	3	3	4	5	26	2	3	5	7	33	0	1	1	2	09
$RuBr_3$	3	4	4	6	32	3	3	4	5	26	2	2	5	7	33	0	1	1	2	09
Ampicillin/ Fluconazole	15	17	18	19	100	15	17	18	19	100	16	17	17	21	100	16	17	17	21	100

Zone of inhibition excludes bore size and zone of inhibition of control, na = not active: error $-1 \leq 0 \leq +1$.

5.1. *Antibacterial activity*

Ligands and their complexes exhibited varying inhibitory effect toward the bacterial strains. The complexes were not sensitive toward Gram-positive bacteria, *S. aureus* and *B. aureus* while they were active against Gram-negative bacteria, *E. coli* and *S. typhi*. In general, metal complexes showed better activity than the corresponding free ligands [35]. Antibacterial activity increased with increasing concentration of the test solution. The enhancement of activity on complexation can be explained by chelation theory and/or Overtone's concept [36–38]. $[RuCl_3L^2]$ exhibited highest activity against *E. coli* while $[RuBr_3L^2_2]$ showed lowest activity and $[RuCl_3L^3]\cdot H_2O$ was not sensitive toward *E. coli*. The activity of the ligands and the complexes were lower than ampicillin. The data indicated that the compounds were less sensitive toward *S. typhi*. L^3, $[RuCl_3L^4]$, $[RuBr_3L^4_{1.5}]\cdot 3H_2O$, and $[RuCl_3L^5]$ were not active against *S. typhi* whereas $[RuBr_3L^2_2]$ exhibited better activity compared to other complexes and uncoordinated ligands. Chloro complexes exhibited higher activity against *E. coli* than bromo analogs except for complexes of L^5.

5.2. *Antifungal activity*

All the compounds were screened for antifungal activity against *C. albicans* and *A. niger*. $[RuCl_3L^5]$ and $[RuBr_3L^5_{1.5}]\cdot 5H_2O$ showed higher activity against *C. albicans* while L^5 showed minimum activity. $[RuBr_3L^2_2]$ exhibited higher activity against *C. albicans* compared to all the other compounds. In general, the inhibition activity against *C. albicans* was slightly augmented by bromide in comparison to chloride. The complexes exhibited inhibition activity, but it did not reach the effectiveness of the standard drug. L^1, L^3, L^4, and L^5 were not sensitive toward *A. niger* while their complexes showed some activity. $[RuCl_3L^2]$ did not inhibit the growth of *A. niger* while L^2 and $[RuBr_3L^2_{1.5}]$ exhibited higher activity. The antifungal activity data indicated that the ligands were less sensitive toward the antifungal activity while it enhanced upon complexation.

The Ru(III) complexes of benzimidazole derivatives showed higher antimicrobial activities than their corresponding ligands but less than standard drugs. Similar behavior was found for bridged ruthenium(III) binuclear complexes by others [27, 39–41]. Binuclear ruthenium(III) complexes of thiobis(β-diketonates), 5-nitro-o-phenanthroline, bis-β-diketones, and 2-fluorophenyl imines showed higher antibacterial or antifungal activity as compared to their parent ligands but did not reach the effectiveness of the respective standard drugs. The increase in activity on complexation was explained on the basis of chelation theory/Overtone's concept/modern electronic theory [36, 42–45].

Acknowledgments

The authors wish to thank VGST, Department of Science and Technology, Government of Karnataka for the "CESEM" award grant No. 24 (2010-11), STIC,

Cochin University for elemental analysis and TGA, SAIF, IIT, Bombay for ESR spectra, Central Instrumentation Facility, Pondicherry University for far-IR spectra, Indian Institute of Science (IISc.), Bangalore for variable temperature magnetic susceptibility measurements, and Spectroscopy/Analytical Test Facility, IISc., Bangalore for ESI-MS. Roopashree thanks JSSATE, Bangalore and JSSMVP, Mysore for encouraging doctoral studies.

References

[1] J.B. Wright. *Chem. Rev.*, **48**, 397 (1951).
[2] P.N. Preston. *Benzimidazole and Congeneric Tricyclic Compounds*, Part-2, Wiley, New York (1980).
[3] N. Boani, M. Gonzalaz. *Mini-Rev., Med. Chem.*, **5**, 409 (2005).
[4] C.S. Allardyce, P.J. Dyson. *Platinum Met. Rev.*, **45**, 62 (2001).
[5] S. Neidle, E.L. Rayner, I.J. Simpson, N.J. Smith, J. Mann, A. Baron, Y. Opoku-Boahen, K.R. Fox, J.A. Hartley, L.R. Kelland. *Chem. Commun.*, 929 (1999).
[6] L. Li, Y.-S. Wong, T. Chen, C. Fan, W. Zheng. *Dalton Trans.*, **41**, 1138 (2012).
[7] D. Thangadurai, S.-K. Ihm. *Transition Met. Chem.*, **29**, 189 (2004).
[8] K.M. Sung, S. Huh, M.J. Jun. *Polyhedron*, **18**, 469 (1999).
[9] D. Chatterjeea, A. Mitra, B.C. Roy. *J. Mol. Catal. A: Chem.*, **161**, 17 (2000).
[10] A.S. Goldstein, R.H. Beer, R.S. Drago. *J. Am. Chem. Soc.*, **116**, 2424 (1994).
[11] M.M.T. Khan, A.E. Martell. *Homogeneous Catalysis of Metal Complexes*, Vol. 1, Academic Press, New York, NY (1974).
[12] A.M. El-Hendawy, S.Y. Alqaradawi, H.A. Al-Madfa. *Transition Met. Chem.*, **25**, 572 (2000).
[13] M.B. Robin, P. Day. *Adv. Inorg. Chem. Radiochem.*, **10**, 247 (1967).
[14] I.W. Hein, R.I. Arhum, J.J. Liquitt. *J. Am. Chem. Soc.*, **79**, 427 (1957).
[15] D.D. Perrin, W.L.F. Armarego, D.R. Perrin. *Purification of Laboratory Chemicals*, 1st Edn, Pergamon Press, Oxford (1966).
[16] W.J. Geary. *Coord. Chem. Rev.*, **7**, 81 (1971).
[17] S. Yurdakul, M. Kurt. *J. Mol. Struct.*, **650**, 181 (2003).
[18] K. Nakamoto. *Infrared and Raman Spectra of Inorganic and Coordination Compounds*, 4th Edn, Wiley Interscience, New York, NY (1986).
[19] A.J. Broomhead, L.A.P. Kane-Maguire. *J. Chem. Soc. (A)*, 546 (1967).
[20] Z. Harzion, G. Navon. *Inorg. Chem.*, **19**, 2236 (1980).
[21] M. Sonmez, M. Celebi, A. Levent, I. Berber, Z. Senturk. *J. Coord. Chem.*, **63**, 1986 (2010).
[22] M.M.T. Khan, D. Srinivas, R.I. Kureshy, N.H. Khan. *Inorg. Chem.*, **29**, 2320 (1990).
[23] T.D. Thangadurai, S.-K. Ihm. *Transition Met. Chem.*, **29**, 189 (2004).
[24] A.B.P. Lever. *Inorganic Electronic Spectroscopy*, 2nd Edn, Elsevier, New York, NY (1989).
[25] M.S. Refat, S.A. El Korashy, D.N. Kumar, A.S. Ahmed. *Spectrochim. Acta, Part A*, **70**, 898 (2008).
[26] S. Kar, N. Chanda, S.M. Mobin, A. Datta, F.A. Urbanos, V.G. Puranik, R. Jimenez-Aparicia, G. Kumar Lahiri. *Inorg. Chem.*, **43**, 4911 (2004).
[27] R. Karvembu, C. Jayabalakrishnan, K. Natarajan. *Transition Met. Chem.*, **27**, 574 (2002).
[28] R. Ramesh, K. Natarajan. *Indian J. Chem.*, **34A**, 535 (1995).
[29] M. Kato, H.B. Jonassen, J.C. Fanning. *Chem. Rev.*, **64**, 99 (1964).
[30] B. Roopashree, V. Gayathri, H. Mukund. *J. Coord. Chem.*, **65**, 1354 (2012).
[31] P.T. Manoharan, P.K. Mehrotra, M.M. Taqui Khan, R.K. Andal. *Inorg. Chem.*, **12**, 2753 (1973).
[32] R.M. Silverstein, G.C. Bassler, T.C. Morril. *Spectroscopic Identification of Organic Compounds*, 4th Edn, Wiley, Singapore (1981).
[33] Y. Wang, G.-W. Lin, J. Hong, L. Li, Y.-M. Yang, T. Lu. *J. Coord. Chem.*, **63**, 3662 (2010).
[34] S. Kaizaki, Y. Kato-lgawa, T. Tsukuda, M. Nakano. *J. Coord. Chem.*, **63**, 967 (2010).
[35] R. Nagar. *Inorg. Biochem.*, **40**, 349 (1990).
[36] Y. Anjaneyula, R.P. Rao. *Synth. React. Inorg. Met. Org. Chem.*, **26**, 257 (1986).
[37] D.M. Taylor, D.R. William. *Trace Element Medicine and Chelation Therapy*, Royal Society of Chemistry, London (1988).
[38] Z.H. Chohan, K.M. Khan, C.T. Supwan. *Appl. Organomet. Chem.*, **18**, 305 (2004).
[39] S.N. Shukla, P. Gaur, R. Mehrotra, M. Prasad, H. Kaur, M. Prasad, R.S. Srivastava. *J. Coord. Chem.*, **62**, 2556 (2009).

[40] N. Padma Priya, S.V. Arunachalam, N. Sathya, V. Chinnusamy, C. Jayabalakrishnan. *Transition Met. Chem.*, **34**, 437 (2009).
[41] S.C.S. Jadon, C. Saxena, R.V. Singh. *Transition Met. Chem.*, **22**, 385 (1997).
[42] B.G. Tweedy. *Phytopathology*, **55**, 910 (1964).
[43] L. Mishra, V.K. Singh. *Indian J. Chem.*, **32A**, 446 (1993).
[44] R. Malhotra, S. Kumar, K.S. Dhindsa. *Indian J. Chem.*, **32A**, 457 (1993).
[45] H. Gilman. *Organic Chemistry: An Advanced Treatise*, Wiley, New York, NY (1943).